

Exact results for surface deposition with precursor layer diffusion

This article has been downloaded from IOPscience. Please scroll down to see the full text article.

1997 J. Phys. A: Math. Gen. 30 3449

(<http://iopscience.iop.org/0305-4470/30/10/021>)

View [the table of contents for this issue](#), or go to the [journal homepage](#) for more

Download details:

IP Address: 171.66.16.71

The article was downloaded on 02/06/2010 at 04:19

Please note that [terms and conditions apply](#).

Exact results for surface deposition with precursor layer diffusion

G J Rodgers^{†§} and J A N Filipe^{‡||}

[†] Department of Physics, Brunel University, Uxbridge, Middlesex, UB8 3PH, UK

[‡] Biomathematics and Statistics Scotland, The University of Edinburgh, JCMB, The King's Buildings, Edinburgh EH9 3JZ, UK

Received 20 November 1996, in final form 26 February 1997

Abstract. An accelerated random sequential adsorption process is studied as a model of chemisorption on a line with precursor layer diffusion. In this process if the position first selected for deposition is occupied then the particle diffuses and is absorbed on the first vacant position it visits. For k -mer deposition exact results are obtained for the gap distribution function. Physically measurable quantities such as the average island size and the probabilities of island nucleation, growth and coagulation are calculated as a function of coverage and the saturation coverage is calculated as a function of k . The continuum version of this model is also considered and potential applications of the models are discussed.

1. Introduction

Random sequential adsorption (RSA) is a process in which particles are adsorbed sequentially and without overlap onto randomly chosen positions on a surface [1–4], once deposited a particle cannot diffuse or desorb from the surface, so adsorption is irreversible. This model is adequate for describing deposition processes in which particles, in a gas or solution, adhere strongly to a surface but interact weakly with each other, apart from being impenetrable. In particular, desorption should be negligible and any diffusion on the substrate should be very slow on the time scale of the observations.

Despite its simplicity, the model has been used to successfully describe the adsorption of colloid particles [5] and gas molecules [6] onto solid surfaces. A virtue of this model is that it is exactly solvable in one dimension in both its lattice and continuum versions [1–4]. On a lattice, k -mers can be deposited in discrete positions along a line [1–3]. In the continuum model [4], known as the *random car parking problem*, cars of length 1 are deposited on an infinite continuous line. The jamming limit, when all the empty spaces are of lengths less than k for the lattice, or less than 1 for the continuum, is reached in an infinite time. To make the model more realistic and to widen its range of applications, various extensions and generalizations of RSA have been proposed and analysed. The inclusion of diffusional relaxation on the substrate [7–9], leading to equilibration, and the possibilities that the particles are reflected back to the fluid or desorbed [9–11] have been examined. The RSA of mixtures of objects of different shapes [12] and of long segments [13] in bi-dimensional lattices has also been considered. Many other studies are detailed in a recent review [14].

§ E-mail address: g.j.rodgers@brunel.ac.uk

|| E-mail address: joao@bioess.sari.ac.uk

Experimental measurements of adsorption kinetics in many gas–metal surfaces [15, 16] have shown that the sticking (or adsorption) probability is largely insensitive to the increase in the *coverage fraction* over a wide range of coverages. This has provided evidence for the existence of more complicated deposition mechanisms. As gas particles approach the surface and lose just enough of their kinetic energy they can become trapped (*physisorbed*) in a mobile, temporary state. The particles can diffuse on the surface in this *precursor state* until they become adsorbed (*chemisorbed*) at a site at a later time. The mechanism of precursor-mediated chemisorption, first postulated by Taylor and Langmuir [17], was formulated as a statistical model in the seminal work of Kisliuk [18]. This was later adapted by King and co-workers [6, 11, 16, 19] to include other physical features. Variations on the Kisliuk model have also been studied by other authors, both numerically and analytically [10, 20–23]. Most analytical treatments, however, are essentially mean-field-like, as they largely ignore the spatial correlations generated by the precursor-mediated deposition process. The importance of the correlations between adatoms had already been recognized by Kisliuk [18], but ignored for mathematical simplicity.

In order to make analytical progress and to gain quantitative insight into the changes induced by precursors in the kinetics of adsorption, a simplified, but non-trivial version of the Kisliuk model was introduced by the present authors in [24], and studied in one dimension. We examined the case where physisorption is only possible on the top of chemisorbed particles, (in *extrinsic precursor states*), and where there is no desorption back to the gas phase. In this model, monomer deposition is attempted sequentially at random sites on a lattice. If the site is occupied, the particle diffuses on top of the occupied region until it reaches a vacant position where it adsorbs irreversibly. It was assumed that the diffusion time scale is small enough compared with the time scale of the deposition trials (i.e. that the process is adsorption limited). This is a plausible assumption if the flux of gas particles onto the surface is low, except in the limit when the surface is almost full (see [24] for a more detailed discussion). Hence, particles in the precursor layer diffuse, with negligible interaction, with one another. Under these conditions, the one-dimensional random walk performed in the precursor state can be effectively modelled by a random choice between adsorption at the left or right edges of the island on which the particle has landed. Note that allowing physisorption on top of the empty sites (*intrinsic precursor states*) implies the existence of interactions between precursor and chemisorbed particles [10], which would complicate the analysis considerably.

As each deposition attempt results in a direct or diffusion-mediated occupation of an empty site the *surface coverage*, θ , grows linearly with time and the *sticking probability* is 1. This represents the limiting behaviour observed in the most common gas–solid systems (see, e.g. [6, p 56]). As a result, the system saturates, with no further deposition possible, after a finite time proportional to the lattice size; full coverage, $\theta = 1$, is reached in the case of monomer deposition. This situation contrasts with conventional RSA, where the time dependence of the coverage is nonlinear and the saturation time is infinite [14]. Since the time dependent behaviour of the coverage is different in the two models, a comparison of physical quantities, such as the average island size, must be carried out as a function of coverage. Another consequence of the (extrinsic) precursor diffusion, which at later times is the dominant mechanism of deposition, is that the edges of islands are preferential sites for chemisorption, especially those of the larger islands. Long-range correlations in the spatial distribution of the adsorbed particles develop, since, as time progresses the precursor particles migrate for larger and larger distances with ever increasing probability. This structuring makes the calculation of the probability distribution of the island sizes, even for monomer deposition in one dimension, highly non-trivial. In [24], approximate

solutions (based on truncation schemes analogous to those employed in [25]) were found to exact equations for the evolution of the island size. These were compared with numerical simulations.

In this paper, further progress is reported. We calculate exactly the probability distribution for the size of inter-island gaps. From this, exact expressions are obtained for several physical properties as a function of time. These include the probabilities per unit time of nucleation, growth and coagulation, the average island size, and the island number density, which were evaluated approximately in [24]. In addition, a k -mer generalization of the model is introduced, and the same quantities are calculated exactly using a similar method. To our knowledge, this is the first study providing a quantitative insight into the dependence of adsorption processes with precursors on the size of the deposited particles. A continuum version of the model is also introduced and solved. A comparison between this model and the standard RSA is made both on a lattice and on the continuum. Following [24], Ben-Naim and Krapivsky [26] recently analysed a one-dimensional generalization of a nucleation-and-growth process, known as the Kolmogorov–Avrami–Johnson–Mehl model, in which the rate of island growth is proportional to the island size rather than being constant. The model is similar to the continuous version of the model studied here, the essential difference being that nucleation occurs in the form of infinitesimal seeds. The surface coverage, in particular, was also found to grow linearly with time. In [26] the model introduced by us in [24] was called an *accelerated RSA* (ARSA) process, a terminology we have adopted here.

One of our motivations for studying the ARSA model was to provide an insight into the role of precursors in chemisorption. In addition, it was suggested by Cassuto and King [19] that a kinetic deposition model without intrinsic precursors and with negligible desorption could explain the experimental data from gas–solid systems such as hydrogen on tungsten. Another, more general motive concerns one of the unrealistic assumptions of the RSA model, that once a deposition trial fails due to overlap, the particle is rejected and the site of the next event is totally uncorrelated to the previous. In real processes, however, where transport to the surface is diffusive, such an event would probably be followed by a nearby adsorption attempt [27]. The ARSA model goes some way towards capturing this feature, especially at lower coverages when the precursor-diffusion length is relatively small. In this respect, the ARSA model is related to previous models in one [28] and two [29] dimensions, aimed at incorporating the effect of local rearrangement due to gravity (rather than due to bulk diffusion). In [29], when a disk contacts a previously adsorbed particle it rolls over that particle along the path of steepest descent; if in the next stable position the particle touches the substrate it sticks, otherwise it is rejected. The configurations obtained in this way are slightly more closely packed than their RSA counterparts.

The essential difference between ARSA and standard nucleation-and-growth models is that the rate of growth of a domain, of a new phase or species, is proportional to its ‘area’, i.e. the rate of occupation of a neighbouring site is proportional to the domain’s linear size. Here, a connection can be made between the ARSA model and, for example, the *contact process* [30] with a nucleation source [31], where the growth rate of a domain is proportional to its ‘perimeter’, i.e. the rate of occupation of a neighbouring site is constant. The occurrence of such exponential growth implies the existence of some long-range transport mechanism whereby the boundary feels effects caused by all elements in the domain. This special form of nucleation-and-growth, or seeding and spreading phenomena is not restricted to molecular and macromolecular surface-adsorption processes. There are other potential applications of the ARSA model, and extensions thereof, in physical and biological systems. One area of application is epidemiology. The model could describe the spatio-temporal spread of

infectious diseases in cases where, for example, the rate at which a susceptible becomes infected is determined by the infection challenge from successive contacts with individuals in a neighbouring infected cluster [32]. Another relevant area is population dynamics, and ecology in particular. Here, local aggregates, or communities, would be seeded and expand due to the internal pressure and dynamics resulting from the creation of offspring and competition for space and resources. It is also conceivable that ARSA could describe the slow deposition of liquid droplets on a plane surface, i.e. the formation and spreading of ‘rain’ puddles, especially on nearly one-dimensional surfaces. The motion of a puddle boundary would result from the imbalance between surface tension and outward pressure waves generated by deposition droplets.

This paper is organized as follows. In section 2, the monomer deposition model is considered and then in section 3 the more general problem of k -mer deposition. Quantities that characterize the island distribution and that can be obtained from the gap size probability distribution, such as the average island size and number, are discussed in section 4. In section 5 a continuum version of the ARSA model is introduced and then finally in section 6 the paper is briefly summarized and some possible extensions to this work are suggested.

2. Monomer deposition

Every chain of empty sites, or gap, is bordered by two chains of occupied sites or islands and vice versa. If a particle lands on one of these islands then it will destroy the gap to the left or the right of the island by diffusing on top of the island before moving into one of the empty sites adjacent to the island. To make progress analytically we must adopt the working hypothesis that the size of the island is uncorrelated with the size of the neighbouring gap. A gap adjacent to a large island is more likely to be destroyed by diffusion than a gap adjacent to a small island. However, the probability that a gap is adjacent to a large island is independent of the size of the gap. This is because the diffusion mechanism only effects the probability of occupation of the sites at the end of the gap, independent of the number of sites in the gap. This hypothesis is confirmed by numerical simulations of the system; the probability distribution of the size of islands next to a 1-gap is the same as that for a 2-gap, 3-gap etc.

Thus, all gaps are destroyed by the diffusion mechanism with a rate proportional to the average island size.

Consequently, the density of gaps of length r , $c_r(t)$ obeys the differential equation

$$\frac{dc_r(t)}{dt} = -rc_r(t) + 2 \sum_{s=0}^{\infty} c_{r+s+1}(t) + q(t)(c_{r+1}(t) - c_r(t)) \quad (1)$$

where time, t , stands for the number of deposition events divided by the system size. Similarly, by ‘density’ we mean the number of occurrences (in this case of finding a gap of size r) divided by the system size. The first term on the right-hand side represents the destruction of a gap of length r by direct deposition. The second term is the creation of a gap of size r by direct deposition in a gap of length $r + s + 1$. The last term corresponds to the creation and destruction of gaps of length r by the diffusion of particles on previously occupied sites. The quantity $q(t)$ is the average island size at time t and is given by

$$q(t) = \frac{\theta(t)}{\sum_{r=1}^{\infty} c_r(t)} \quad (2)$$

where the term in the denominator is equal to the total number density of islands and the

coverage is given by

$$\theta(t) = 1 - \sum_{r=1}^{\infty} r c_r(t). \quad (3)$$

If we set $q = 0$ the equation describes the RSA of monomers on a chain. Even though it is nonlinear, equation (1) can be solved, self-consistently, using the method developed in [33]. We anticipate a solution with the form

$$c_r(t) = A(t) \exp\{-rt\} \quad (4)$$

with initial conditions, as in [33], $c_r(0) = 0$ and

$$\lim_{t \rightarrow 0} \sum_{r=1}^{\infty} r c_r(t) = 1. \quad (5)$$

This latter condition implies that

$$\lim_{t \rightarrow 0} \frac{A(t)}{t^2} = 1. \quad (6)$$

Inserting (4) into (2) and (3) gives

$$q(t) = \frac{1 - e^{-t}}{A(t)e^{-t}} - \frac{1}{1 - e^{-t}} \quad (7)$$

and (4) into (1) gives

$$\frac{dA(t)}{dt} = A(t)q(t)(e^{-t} - 1) + 2A(t) \frac{e^{-t}}{1 - e^{-t}}. \quad (8)$$

Eliminating $q(t)$ between these two equations gives a differential equation for $A(t)$ which can be solved, subject to the initial condition (6), to reveal

$$c_r(t) = (1 - t)e^t (1 - e^{-t})^2 e^{-rt}, \quad (9)$$

$\theta(t) = t$, as expected, and the island density

$$q(t) = \frac{t}{1 - t} \frac{1}{1 - e^{-t}}. \quad (10)$$

To compare the results of this process with those for the RSA of monomers, we consider the probability for island nucleation, coagulation and growth per successful deposition event. We denote these quantities by P_n , P_c and $P_g (= 1 - P_n - P_c)$ respectively. For RSA $P_n = (1 - \theta)^2$ and $P_c = \theta^2$ whereas for this model

$$P_n = \sum_{r=2}^{\infty} (r - 2)c_r(t) = (1 - \theta)e^{-2\theta} \quad (11)$$

and

$$P_c = c_1(t) + \theta(t) \frac{c_1(t)}{\sum_{r=1}^{\infty} c_r(t)} = (1 - e^{-\theta})[1 - (1 - \theta)e^{-\theta}]. \quad (12)$$

Figure 1 contains a graph of P_n , P_c and P_g against θ for the two models. For ARSA, $P_g \rightarrow e^{-1} > 0$ as $\theta \rightarrow 1$, indicating that there are a finite number of gaps with two empty sites at large coverage. The results presented in figure 1 are indistinguishable from the numerical simulations of the ARSA model in [24]. A similar agreement is found for the number density of islands, shown in figure 2.

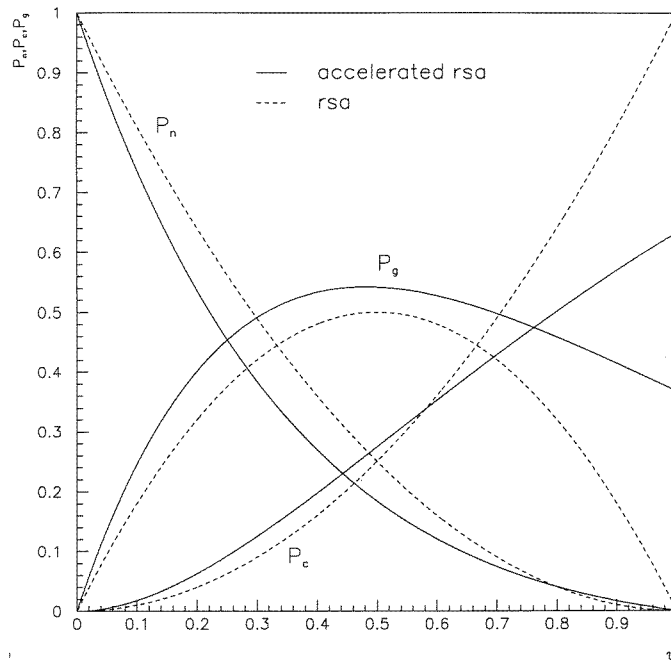


Figure 1. Probabilities of island nucleation, coagulation and growth per successful deposition event as a function of coverage.

3. k -mer deposition

For the deposition of k -mers the analogue of equation (1) is

$$\frac{dc_r(t)}{dt} = -[r - (k - 1)]c_r(t) + 2 \sum_{s=0}^{\infty} c_{r+s+k}(t) + q(t)(c_{r+k}(t) - c_r(t)) \quad (13)$$

for $r \geq k$ and

$$\frac{dc_r(t)}{dt} = 2 \sum_{s=0}^{\infty} c_{r+s+k}(t) + q(t)c_{r+k}(t) \quad (14)$$

for $r < k$. The initial conditions are the same as before (equation (5)). Now $q(t)$ is

$$q(t) = \frac{1 - \sum_{r=k}^{\infty} [r - (k - 1)]c_r(t)}{\sum_{r=k}^{\infty} c_r(t)} \quad (15)$$

and is equal to the average length of the chains of sites in which it is not possible to deposit a k -mer. This is the average length of chain in which a physisorbed particle will diffuse before chemisorption takes place. The denominator contains the number of gaps of lengths greater than k , which is equal to the number of chains in which a k -mer cannot be deposited. The numerator is one minus the total number density of positions in which it is possible to place a k -mer, which is equal to the total number density of positions in which a k -mer cannot be deposited.

In analogue with the monomer model, equations (13) and (14) are solved by

$$c_r(t) = A(t) \exp\{-(r - (k - 1))t\} \quad (16)$$

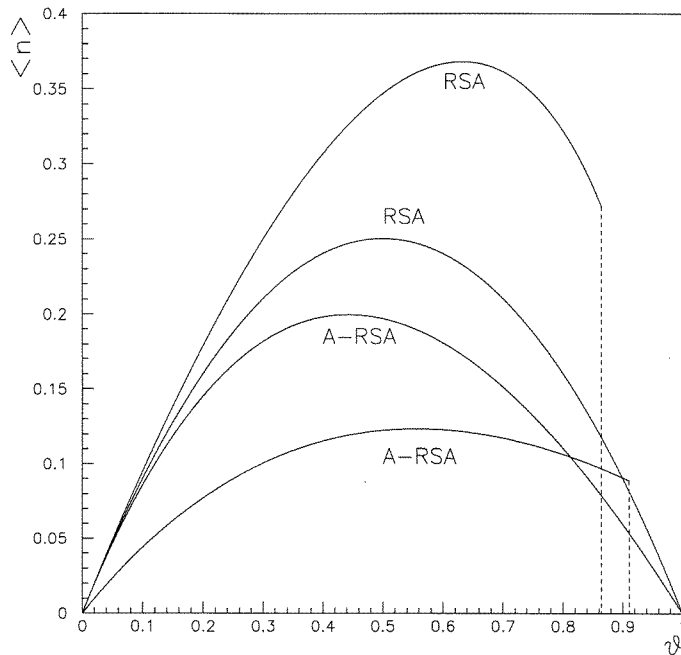


Figure 2. The number density of islands as a function of coverage for the RSA and ARSA models with monomers and dimers. The monomer curves are continuous as $\theta \rightarrow 1$.

for $r \geq k$. Now we have

$$\frac{dA(t)}{dt} = A(t)q(t)(e^{-kt} - 1) + 2A(t)\frac{e^{-kt}}{1 - e^{-t}} \tag{17}$$

and equation (7) for $q(t)$. We can eliminate $q(t)$ between these equations and solve $A(t)$ to reveal

$$c_r(t) = (1 - e^{-t})^2 \left[\frac{2 - \int_0^t du F_k(u)}{F_k(t)} - 1 \right] e^{-(r-k)t} \tag{18}$$

for $r \geq k$ where

$$F_k(t) = \exp \left\{ \int_0^t \frac{1 - e^{-ku}}{1 - e^{-u}} du - t \right\} = \exp \left\{ \sum_{r=1}^{k-1} \frac{1 - e^{-rt}}{r} \right\} \tag{19}$$

and

$$c_r(t) = \int_0^t (1 - e^{-u})e^{-ru} \left[\frac{2 - \int_0^u dv F_k(v)}{F_k(u)} \right] du \tag{20}$$

for $r < k$. It is relatively straightforward to show that this solution gives

$$\theta(t) = kt$$

as we would expect. The critical time at which the line is saturated is the time at which the only gaps are of size $k - 1$ or less. This occurs when $c_r(t_c) = 0$ for all $r \geq k$. This condition can be inserted into (16) to give an equivalent condition, $A(t_c) = 0$, or

$$F_k(t_c) + \int_0^{t_c} du F_k(u) = 2 \tag{21}$$

Table 1. The saturation coverage for the ARSA process as a function of k .

k	$\theta(t_c)$
1	1
2	0.9115...
3	0.8865...
4	0.8747...
5	0.8678...
6	0.8633...
7	0.8601...
8	0.8578...
9	0.8560...
10	0.8545...
100	0.8430...
1000	0.8419...
∞	0.8417...

and hence the saturation coverage $\theta(t_c) = kt_c$. This equation has been solved by using Newton's method to give the saturation coverage as a function of k in table 1. These values have also been confirmed by direct numerical simulation of the system.

A comparison can be made between the saturation coverage for this model and that for the standard RSA model [34]; the ARSA process leads to a higher coverage for $k > 1$ as it has a more efficient packing mechanism. In the limit $k \rightarrow \infty$, with suitable rescaling, one recovers results for the continuum version of this problem, which is introduced in section 5. As in the RSA model, the approach of the saturation coverage to this limit goes like $1/k$ [34].

4. Results

There are a number of statistical quantities of physical interest that can be derived from the gap size probability distributions in the previous two sections. These include the total number of gaps, the number of gaps of lengths greater than or equal to k , and the number of gaps of lengths less than k . One can also study the total length covered by gaps of these three types and, consequently, the average size of each of these gaps. All these quantities are easily obtained from the gap size probability distribution.

Also of interest experimentally is the average island size $\langle L \rangle$ as a function of coverage, which is obtained via the expression

$$\langle L \rangle = \frac{\theta}{\sum_{r=1}^{\infty} c_r(t)} = \theta \left[\int_0^{\theta/k} du e^{-u} \left[\frac{2 - \int_0^u dv F_k(v)}{F_k(u)} \right] - \theta/k \right]^{-1}. \quad (22)$$

For monomer RSA $\langle L \rangle = 1/(1 - \theta)$ whereas for ARSA, we have (with the same $q(t)$ as in (10))

$$\langle L \rangle = \frac{\theta}{(1 - \theta)(1 - e^{-\theta})}. \quad (23)$$

For dimer RSA

$$\langle L \rangle = \frac{2\theta}{(1 - \theta) \log \left(\frac{1}{1 - \theta} \right)} \quad (24)$$

Table 2. The saturation values of $\langle L \rangle/k$ for the ARSA process as a function of k .

k	$\langle L(t_c) \rangle/k$
1	∞
2	5.151
3	3.792
4	3.340
10	2.790
∞	2.436

when $\theta < \theta(\infty) = 1 - e^{-2}$. When $\theta = \theta(\infty)$, $\langle L \rangle = \theta(\infty)/(1 - \theta(\infty)) = e^2 - 1 = 6.389 \dots$, indicating that in the saturated state a typical island contains about three dimers. For the ARSA of dimers,

$$\langle L \rangle = \frac{\theta}{1 - \theta - \exp\{e^{-\theta/2}\} \left[e^{-1} - \int_{e^{-\theta/2}}^1 \frac{1+v}{v} e^{-v} dv \right]} \quad (25)$$

when $\theta < \theta(t_c) = 0.9114 \dots$ and $\langle L \rangle = \theta(t_c)/(1 - \theta(t_c)) = 10.30 \dots$ for $\theta = \theta(t_c)$. This indicates that in the saturated state a typical island contains about five dimers. Table 2 shows the saturation values of $\langle L \rangle/k$ for several values of k .

Notice that as $\theta \rightarrow 0$, $\langle L \rangle \rightarrow 1$ for the monomer deposition models and two for the dimers. These are special cases of a general result for k -mer deposition, $\langle L \rangle \rightarrow k$ as $\theta \rightarrow 0$, which follows from (22). This indicates that for short times the few particles that have been deposited are in isolated islands.

Figure 2 contains a graph of the number density of islands ($\langle n(\theta) \rangle$) as a function of coverage for the RSA and ARSA of both monomers and dimers. This is simply related to the average island size by $\langle L(\theta) \rangle = \theta/\langle n(\theta) \rangle$. In addition, the nearest-neighbour correlation function is given by the difference $\theta - \langle n(\theta) \rangle$ [24]. For a given coverage the number of islands for the RSA process is greater than that for ARSA, a consequence of the more efficient packing mechanism in ARSA.

5. Continuum deposition

In the RSA continuum problem on a line [4, 33], cars of length 1 are placed at randomly chosen positions. If the position chosen is partially occupied then no deposition takes place. Here we consider the accelerated version of this model; when a deposition attempt is unsuccessful, the car diffuses along the line before parking in the first vacant space it comes to that is large enough to take it. In this case the car parks so that it is touching the last car it drove past. This mechanism is illustrated in figure 3. The kinetic equation for the gap size distribution $c(x, t)$ of this *accelerated random car parking problem* is

$$\frac{\partial c(x, t)}{\partial t} = -(x - 1)c(x, t) + 2 \int_{x+1}^{\infty} c(y, t) dy + q(t)[c(x + 1, t) - c(x, t)] \quad (26)$$

for $x \geq 1$ and

$$\frac{\partial c(x, t)}{\partial t} = 2 \int_{x+1}^{\infty} c(y, t) dy + q(t)c(x + 1, t) \quad (27)$$

for $0 < x < 1$.

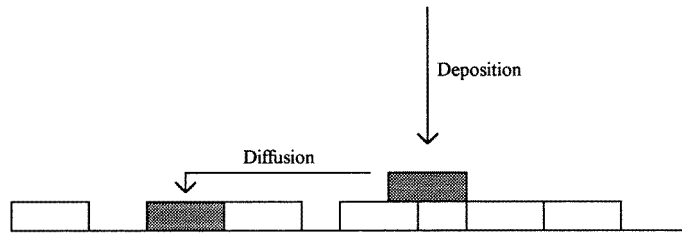


Figure 3. The diffusion mechanism in the continuum ARSA model.

Equations (26) and (27) are similar to that for the accelerated Kolmogorov–Avrami–Johnson–Mehl nucleation-and-growth process studied in [26]. These equations will give the continuous part of the gap size probability distribution. The introduction of precursor diffusion into this model results in a Dirac δ -function at $x = 0$ in the gap distribution associated with the cars that diffuse and are deposited in a position touching a neighbouring car. The amplitude of this δ -function can be calculated as a function of θ but is not of any particular interest. In the conventional RSA problem cars are never deposited touching one another so in RSA a new gap is created at every successful deposition whereas in ARSA this is not the case.

In equations (26) and (27), $q(t)$ is the average length of chain in which it is not possible to deposit a car of length 1,

$$q(t) = \frac{1 - \int_1^\infty (y-1)c(y,t) dy}{\int_1^\infty c(y,t) dy}. \quad (28)$$

These equations can be solved in a similar way to the lattice model, to reveal $\theta(t) = t$,

$$c(x,t) = t^2 [2 \exp\{-G(t)\} - 1] \exp\{-(x-1)t\} \quad (29)$$

for $x > 1$ and

$$c(x,t) = 2 \int_0^t u \exp\{-xu - G(u)\} du \quad (30)$$

for $x < 1$ where

$$G(t) = \int_0^t \frac{1 - e^{-v}}{v} dv. \quad (31)$$

The saturation coverage ($\theta(t_c) = t_c$) is given by the condition $c(x, t_c) = 0$ for $x > 1$. Using (28) gives $G(t_c) = \ln 2$ and hence that $\theta(t_c) = 0.8416\dots$. As we mentioned in section 3, this result can be obtained by taking the limit $k \rightarrow \infty$ after suitable rescaling of (21); the integral term in (21) vanishes, while $F_k(t) \rightarrow \exp\{G(t)\}$. It is also easy to show, by taking the same limit under appropriate rescaling, that (29) and (30) follow from (18) and (20), and that $\langle L \rangle/k$ (where $\langle L \rangle$ is given by (22)) tends to

$$\langle L \rangle = \frac{t}{2 \int_0^t du e^{-G(u)} - t} \quad (32)$$

which is equal to

$$\frac{t}{\int_0^\infty dx c(x,t)}. \quad (33)$$

This can be used to calculate the mean number of (touching) cars per island at saturation, which we find to be 2.436...

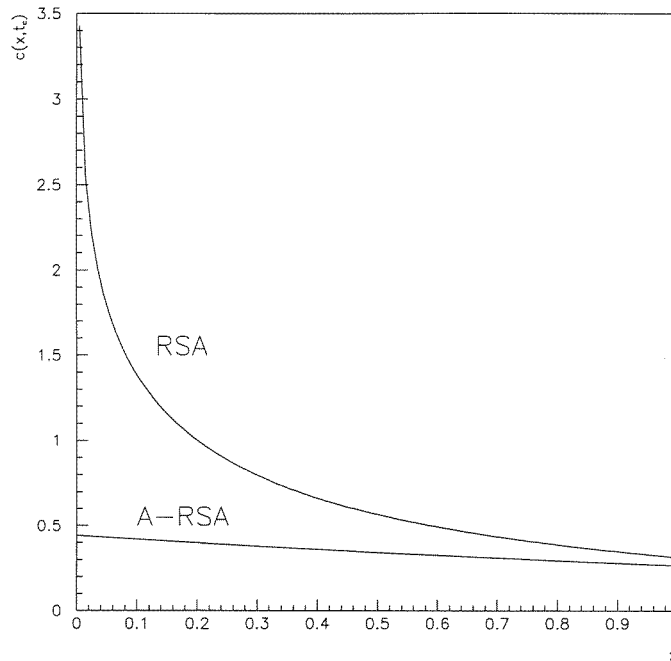


Figure 4. The gap number distribution in the saturation limit for the continuum RSA and ARSA model.

Using (30) one can show that the distribution of empty spaces at saturation is given by

$$c(x, t_c) = 2 \int_0^{t_c} u \exp\{-xu - G(u)\} du \quad (34)$$

with t_c determined by $G(t_c) = \ln 2$. This can be compared with the equivalent quantity for RSA [4, 33]

$$c(x, \infty) = 2 \int_0^{\infty} u \exp\{-xu - 2G(u)\} du. \quad (35)$$

Figure 4 contains a graph of these two number distributions. Notice that as $x \rightarrow 0$ the distribution for RSA diverges logarithmically whereas that for ARSA tends to a constant value. This difference arises from the difference in the late stage kinetics. When the coverage is close to its saturation value, in RSA the kinetics comprise of the filling of gaps which are of a size only just greater than 1. In ARSA these gaps are filled by the diffusion mechanism which does not create small gaps at the same rate. It would be interesting to see if different deposition rules could give other types of divergence in $c(x, t_c)$ as $x \rightarrow 0$.

The number distributions (34) and (35), in figure 4, do not have the same normalization. This is because they are normalized to the total number of empty spaces at saturation, which is different in the two models. The curve for the ARSA model appears to be a straight line when plotted with the standard RSA curve. It is in fact quite curved, although not as profoundly as that for RSA.

6. Summary and conclusions

We have derived exact results in one dimension for the ARSA model introduced in [24] describing surface deposition with precursor-layer diffusion.

As time progresses, nucleation becomes less frequent and the precursor-mediated deposition mechanism dominates (figure 1). During this process, the larger islands grow and coalesce more rapidly and the precursor particles tend to migrate for longer and longer distances, establishing correlations between sites further and further apart. These long-range correlations generate a non-trivial distribution of island sizes, which was calculated approximately in [24]. An exact calculation of the gap-size distribution is possible, however, because the size of the inter-island gaps remains uncorrelated to the size of the adjacent islands. As a result, statistical quantities describing the island pattern that only depend on the island-gap interface, such as the island number density and average size, can be calculated exactly. Perfect agreement was found with numerical simulations of the system.

An ARSA model with k -mer deposition on a line was introduced and analysed using the same method. Here, in addition to the previous quantities, the saturation coverage (table 1) was calculated as a function of k . This study allowed an understanding of how the size of the deposited particles affects the ARSA process. In the case of molecular adsorption, the model mimics the geometric effects resulting from changing the size of the molecules relative to the microscopic structure of the substrate. In the case of the population dynamics model mentioned in the introduction, for example, k accounts for the minimum amount of space and resources required by an individual to survive. The typical number of molecules in a cluster, or of individuals in a population aggregate, is given by $\langle L(t) \rangle / k$, whose saturation value is given in table 2. While the average island size increases with k , and accordingly the island number density decreases, the average number of touching particles in a row decreases with k .

A continuum model for ARSA, an *accelerated random car parking problem*, was also introduced and solved. This describes the situation where there are no constraints on the positions available in the empty regions of the substrate. As expected, all the results agree with those for k -mer deposition on a lattice in the limit $k \rightarrow \infty$.

The results for ARSA were also compared with those for conventional RSA. Since the precursor-diffusion mechanism is much more effective than direct deposition in filling up the substrate, in ARSA there are a smaller number of islands for a given coverage than in RSA (figure 2). Correspondingly, more closely packed saturation configurations are reached in k -mer and continuous ARSA (table 1) than in their RSA counterparts. The saturation limit of the gap-size distribution was shown to be more uniform for continuous ARSA than for continuous RSA; in the latter case it diverges at the origin (figure 4). This is consistent with the observation that in monomer ARSA the probabilities of growth and coalescence tend to non-trivial values as $\theta \rightarrow 1$, while $P_g \rightarrow 0$ and $P_c \rightarrow 1$ in monomer RSA (figure 1). Conversely, the island-size distribution was found to peak at the origin in monomer ARSA, while being more uniform in monomer RSA [24].

There are a number of possible extensions to this work. One of these is to consider the deposition of a mixture of particles with different sizes. This corresponds to the situation where different molecules, or species compete to occupy the space available. The model can also be generalized by allowing only a fraction of the incident molecules, or offspring, to be energetically capable of diffusing in the precursor layer. In this case the coverage grows nonlinearly with time [24]. Another possibility is to allow deposited particles to diffuse in the empty spaces. A one-dimensional problem like this, but without extrinsic precursor diffusion, has recently been solved exactly [35]. The application of ARSA models, and

related ones to studying epidemic spread is also being considered [32].

Acknowledgments

JANF thanks the Scottish Office Agricultural and Fisheries Department for partial financial support of this work. We would both like to thank Gavin Gibson and Kamrul Hassan for valuable remarks on the manuscript.

References

- [1] Widom B 1963 *J. Chem. Phys.* **44** 3888
Widom B 1973 *J. Chem. Phys.* **55** 4043
- [2] Flory P J 1939 *J. Am. Chem. Soc.* **61** 1518
- [3] Cohen E R and Reiss H 1963 *J. Chem. Phys.* **38** 680
- [4] Renyi A 1958 *Publ. Math. Inst. Hung. Acad. Sci.* **3** 109
- [5] Senger B, Voegel J C, Schaaf P, Johner A, Schmitt A and Talbot J 1991 *Phys. Rev. A* **44** 6926
Senger B, Voegel J C, Schaaf P, Johner A, Schmitt A and Talbot J 1992 *J. Chem. Phys.* **97** 3813
- [6] Morris M A, Bowker M and King D A 1984 *Comprehensive Chemical Kinetics* vol 19, ed C H Bamford, C F H Tipper and R G Compton (Amsterdam: Elsevier) ch 1
- [7] Bartelt M C and Evans J W 1992 *Phys. Rev. B* **46** 12 675
- [8] Privman V and Barma M 1992 *J. Chem. Phys.* **97** 6714
- [9] Tarjus G, Schaaf P and Talbot J 1990 *J. Chem. Phys.* **93** 8352
- [10] Hood E S, Toby B H and Weinberg W H 1985 *Phys. Rev. Lett.* **55** 2437
- [11] King D A 1977 *Surf. Sci.* **64** 43
- [12] Barker G C and Grimson M J 1988 *J. Mol. Phys.* **63** 145
- [13] Bonnier B, Hontebeyrie M, Leroyer Y, Meyers C and Pommiers E 1994 *Phys. Rev. E* **49** 305
- [14] Evans J W 1993 *Rev. Mod. Phys.* **65** 1281
- [15] Tang S L, Lee M B, Beckerle J D, Hines M A and Ceyer S T 1985 *J. Chem. Phys.* **82** 2826
Guo X C, Bradley J M, Hopkinson A and King D A 1994 *Surf. Sci.* **310** 163
- [16] King D A and Wells M G 1974 *Proc. R. Soc. A* **339** 245
- [17] Taylor J B and Langmuir I 1933 *Phys. Rev.* **44** 423
- [18] Kisliuk P 1957 *J. Phys. C: Solid State Phys.* **3** 95
Kisliuk P 1958 *J. Phys. C: Solid State Phys.* **5** 78
- [19] Cassuto A and King D A 1981 *Surf. Sci.* **103** 388
- [20] Wolf N O, Burgess D R and Hoffman D K 1980 *Surf. Sci.* **100** 453
- [21] Becker O M and Ben-Shaul A 1988 *Phys. Rev. Lett.* **61** 2859
- [22] Evans J W 1989 *Phys. Rev. A* **40** 2868
- [23] Evans J W and Nord R S 1987 *J. Vac. Sci. Tech. A* **5** 1040
- [24] Filipe J A N and Rodgers G J 1995 *Phys. Rev. E* **52** 6044
- [25] Nord R S and Evans J W 1985 *J. Chem. Phys.* **82** 2795
- [26] Ben-Naim E and Krapivsky P L 1996 *Phys. Rev. E* **54** 3562
- [27] See, e.g. Schaaf P, Johner A and Talbot J 1991 *Phys. Rev. Lett.* **66** 1603
- [28] Viot P, Tarjus G and Talbot J 1993 *Phys. Rev. E* **48** 480
- [29] Jullien R and Meakin P 1992 *J. Phys. A: Math. Gen.* **25** L189
Tarjus G, Viot P, Choi H S and Talbot J 1994 *Phys. Rev. E* **49** 3239
- [30] Liggett T M 1985 *Interacting Particles* (New York: Springer)
- [31] Filipe J A N and Gibson G J 1997 *Phil. Trans. R. Soc. B* submitted
- [32] Filipe J A N in preparation
- [33] Krapivsky P L 1992 *J. Stat. Phys.* **69** 135
- [34] González J J, Hemmer P C and Høye J S 1974 *Chem. Phys.* **3** 228
- [35] Kartal S and Rodgers G J 1997 *Phys. Lett. A* **225** 239